Hot-electron mobility in laterally confined systems

1994 J. Phys.: Condens. Matter 6 5667

(http://iopscience.iop.org/0953-8984/6/29/009)

J. Phys.: Condens. Matter 6 (1994) 5667–5680. Printed in the UK

Hot-electron mobility in laterally confined systems

X F Wang† and X L Lei†‡

† State Key Laboratory of Functional Material for Informatics, Shanghai Institute of Metallurgy, Chinese Academy of Sciences, 865 Changning Road, Shanghai, 200050, People's Republic of China

‡ China Centre of Advanced Science and Technology (World Laboratory), PO Box 8730, Beijing, 100080, People's Republic of China

Received 18 November 1993, in final form 17 May 1994

Abstract. Hot-electron transport in GaAs/AlGaAs quantum wires and quantum wells having various lateral confinements are investigated systematically using the Lei–Ting balance equation theory. Intrasubband and intersubband transitions of up to 21 electron subbands in quantum wires and seven subbands in quantum wells due to acoustic phonons, optic phonons and impurities are taken into account. Linear and non-linear electron mobilities are presented as functions of carrier density, electron field (or drift velocity), temperature and lateral confinement for these one-dimensional (1D) and two-dimensional (2D) systems, and compared with those in bulk material. At low temperatures, the electron mobility in quantum wires can be much higher than that in quantum wells or in bulk material in optimum conditions. However at high temperatures, when optic phonon scattering dominates the other scattering mechanisms, the mobility in quantum wires can hardly exceed the value in quantum wells or in bulk material.

1. Introduction

Electron transport in semiconductor microstructures, such as quantum wires and quantum wells, has been one of the most interesting objects of study over recent years. The reason for this is twofold. Firstly, new properties in those structures have been extensively exploited to develop high-quality electronic devices. Secondly, the behaviour of carriers in those structures has not yet been fully understood. Electron drift velocity is limited by scattering with impurities and phonons in the material. With the newly developed molecular beam epitaxy (MBE) technology, extremely pure GaAs/AlGaAs heterojunctions, where the effect of impurity on electron transport is strongly suppressed, can be manufactured and electron mobility as high as $\mu \sim 10^3$ m^2 V^{-1} s^{-1} has been observed in two-dimensional electron systems [1]. Long quantum wires of various geometries have been fabricated for transport investigation as well as quantum wells [2–6] and some interesting phenomena, for example electron mobility modulation with electron density [3] and modification of phonon spectrum [6], were observed.

The desire for interpretation and anticipation of phenomena in semiconductor microstructures stimulated the theoretical investigation of low-dimensional electron systems [7]. Electrons in heterojunctions have been investigated extensively in past decades [8–12]. The scattering rate or transport of electrons in the extreme quantum limit (EQL) in both quantum wells and quantum wires have also been calculated by many authors [13–18]. A much higher electron mobility was expected in quantum wires than in quantum wells and bulk material at both low and high temperatures.

0953-8984/94/295667+14$19.50

Recently, interest has been focused on the study of scattering rates or high-field transport including the influence of intersubband transitions in quantum wells and quantum wires [9, 18–27]. The optic phonon dominant transport at high temperatures in quantum wires was investigated using a Monte Carlo method by Brigg and Leburton [22] and Mickevicius and co-workers [27]. The effects of quantum confinement in a special GaAs field effect transistor were discussed by Sernelius and co-workers [23]. Subband effects on electron linear mobility due to electron–impurity interactions in quantum wires with a harmonic lateral potential had been demonstrated by Hu and O'Connell [24]. Phonon-caused scattering rates and energy relaxation including subband effects in low-dimensional electron systems based on InGaAs/InP and AlGaAs/GaAs were discussed by Bockel and co-workers [25] and by Wang and Lei [26] respectively. However, most previous studies only discussed fragmentary transport results of electrons in quantum wells or quantum wires, especially in non-linear cases, and were short of systematic comparisons between electron systems of different dimensionality.

In the present paper, by employing the Lei–Ting balance equation transport theory [28], we systematically investigate the linear and non-linear electron mobility in a wide range of temperature, electric field, carrier density and lateral confinement. Intrasubband and intersubband scattering due to impurities, acoustic phonons (deformation potential and piezoelectric couplings with electrons) and polar optic phonons are taken into account. Subband effects, if of concern, were all included. At low lattice temperature, linear mobility in quantum wires may be much higher than that in bulk material and quantum wells in optimum conditions. At high lattice temperature, or under the influence of high electric field, however, linear and non-linear electron mobilities are on average lower than or close to the values in quantum wells or bulk materials. When the confinement in quantum wells or quantum wires becomes weak, crossover from low-dimensional systems to three-dimensional system can be observed.

2. Balance equations

As to quantum well and wire models, we use a GaAs slab (quantum slab) with a width of d_2 and an area of A, and a GaAs cylinder of diameter d_1 and length L embedded in undoped bulk AlGaAs respectively. Assuming infinitely deep wells, the electron wavefunctions of the quantum slab and quantum wire are

$$\psi^{2D} = \frac{e^{ik_\parallel \cdot r_\parallel}}{\sqrt{A}} \sqrt{\frac{2}{d_2}} \sin\left(\frac{n\pi z}{d}\right) \qquad n = 1, 2, 3, \ldots \tag{1}$$

and

$$\psi^{1D} = \frac{e^{ik_z z}}{\sqrt{L}} C_l^m J_m\left(\frac{2x_l^m}{d_1}\rho\right) e^{im\phi} \qquad \begin{cases} m = \ldots, -1, 0, 1, \ldots \\ l = 1, 2, 3, \ldots \end{cases} \tag{2}$$

with corresponding energies

$$\varepsilon_n^{2D}(k_\parallel) = \varepsilon_n + \frac{k_\parallel^2}{2m^*} = \frac{\pi^2 n^2}{2m^* d_2^2} + \frac{k_\parallel^2}{2m^*} \tag{3}$$

and

$$\varepsilon_{m,l}^{1D}(k_z) = \varepsilon_{m,l} + \frac{k_z^2}{2m^*} = \frac{2(x_l^m)^2}{m^* d_1^2} + \frac{k_z^2}{2m^*}. \tag{4}$$

Here we use spatial coordinates (x, y, z) for the 2D system and (ρ, ϕ, z) for the 1D system, $k_\parallel \equiv (k_x, k_y)$ denotes the parallel wavevector component for the quantum slab and k_z the axial component for the quantum wire; $C_l^m = 2/(\sqrt{\pi} y_l^m d_1)$ is the normalization factor, x_l^m is the lth zero of the mth-order Bessel function, i.e. $J_m(x_l^m) = 0$, and $y_l^m = J_{m+1}(x_l^m)$, and m^* is the effective mass of the electron.

We consider electrons in the quantum slab under the influence of an electric field in the x direction and in the quantum wire under the influence of an electric field along the z direction. Transport properties of these systems are obtained by solving the force- and energy-balance equations of Lei and Ting [9, 26, 28]:

$$eE + f(v_d) = 0 \tag{5}$$

$$v_d f(v_d) + w(v_d) = 0. \tag{6}$$

The frictional force per electron, $f(v_d)$, is given by

$$\begin{aligned} f^{2D}(v_d) = {} & \frac{n_i}{n_3 d_2} \sum_{n,n',q} |U(q)|^2 |F_{n'n}^{2D}(q_z)|^2 q_x \Pi_2^{2D}(n', n, q_\parallel, q_x v_d) \\ & + \frac{2}{n_3 d_2} \sum_{n,n',q,\lambda} |M(q,\lambda)|^2 |F_{n'n}^{2D}(q_z)|^2 q_x \Pi_2^{2D}(n, n', q_\parallel, \Omega_{q\lambda} + q_x v_d) \\ & \times \{n(\Omega_{q\lambda}/T) - n[(\Omega_{q\lambda} + q_x v_d)/T_e]\} \end{aligned} \tag{7}$$

and

$$\begin{aligned} f^{1D}(v_d) = {} & \frac{4n_i}{\pi n_3 d_1^2} \sum_{\substack{m,m' \\ l,l',q}} |U(q)|^2 |F_{m'ml'l}^{1D}(q_\parallel)|^2 q_z \Pi_2^{2D}(m, m', l, l', q_z, q_z v_d) \\ & + \frac{8}{\pi n_3 d_1^2} \sum_{\substack{m,m',l,l' \\ q,\lambda}} |M(q,\lambda)|^2 |F_{m'ml'l}^{1D}(q_\parallel)|^2 q_z \Pi_2^{1D}(m, m', l, l', q_z, \Omega_{q\lambda} + q_z v_d) \\ & \times \{n(\Omega_{q\lambda}/T) - n[(\Omega_{q\lambda} + q_z v_d)/T_e]\} \end{aligned} \tag{8}$$

for quantum slab (2D) and quantum wire (1D) systems respectively. The corresponding energy loss rates per electron $w(v_d)$ are

$$\begin{aligned} w^{2D}(v_d) = {} & \frac{2}{n_3 d_2} \sum_{n,n',q,\lambda} |M(q,\lambda)|^2 |F_{n'n}^{2D}(q_z)|^2 \Omega_{q\lambda} \Pi_2^{2D}(n, n', q_\parallel, \Omega_{q\lambda} + q_x v_d) \\ & \times \{n(\Omega_{q\lambda}/T) - n[(\Omega_{q\lambda} + q_x v_d)/T_e]\} \end{aligned} \tag{9}$$

and

$$\begin{aligned} w^{1D}(v_d) = {} & \frac{8}{\pi n_3 d_1^2} \sum_{\substack{m,m',l,l' \\ q,\lambda}} |M(q,\lambda)|^2 |F_{m'ml'l}^{1D}(q_\parallel)|^2 \Omega_{q\lambda} \Pi_2^{1D}(m, m', l, l', q_z, \Omega_{q\lambda} + q_z v_d) \\ & \times \{n(\Omega_{q\lambda}/T) - n[(\Omega_{q\lambda} + q_z v_d)/T_e]\}. \end{aligned} \tag{10}$$

Here T is the lattice temperature, T_e is the electron temperature, v_d is the average drift velocity, which is always along the electric field direction for the cases discussed here, $\Omega_{q\lambda}$ is the energy of a phonon with 3D wavevector $q \equiv (q_\parallel, q_z)$ in branch λ, $M(q,\lambda)$ and

$U(q)$ are the electron–phonon coupling and electron–impurity scattering matrix in the 3D Fourier representation respectively, n_i is the effective bulk density of impurities, n_3 is the bulk electron density and $n(x) \equiv [\exp(x) - 1]^{-1}$ is the Bose function.

The terms $F^{2D}_{nn'}$ and $F^{1D}_{mm'll'}$ are the form factors of electrons in the quantum well and the quantum wire:

$$|F^{2D}_{nn'}(q_z)|^2 = \left| \frac{4\pi^2 q_z d_2 n n'}{[(q_z d_2)^2 - (n-n')^2\pi^2][(q_z d_2)^2 - (n+n')^2\pi^2]} \right|^2 \times \begin{cases} 2(1-\cos q_z d_2) & \text{for even } n-n' \\ 2(1+\cos q_z d_2) & \text{for odd } n-n' \end{cases} \tag{11}$$

$$|F^{1D}_{mm'll'}(q_\parallel)|^2 = 4\left| \int_0^1 \xi \, d\xi \frac{1}{y_l^m y_{l'}^{m'}} J_m(x_l^m \xi) J_{m'}(x_{l'}^{m'} \xi) J_{|m-m'|}(0.5 q_\parallel d_1 \xi) \right|^2. \tag{12}$$

The terms $\Pi_2^{2D}(n, n', q_\parallel, \omega)$ and $\Pi_2^{1D}(m, m', l, l', q_z, \omega)$ are the imaginary parts of the electron density–density correlation functions in the quantum slab and quantum wire respectively [9, 26, 28]. Neglecting the dynamic screening, they can be expressed as

$$\Pi_2^{2D} = \sqrt{\frac{m^* T_e}{2\pi}} \frac{m^*}{q_\parallel} \left\{ F_{-1/2}\left[\frac{\varepsilon_f - \varepsilon_{n'}}{T_e} - \frac{m^*}{2q_\parallel^2 T_e}\left(\omega + \varepsilon_n - \varepsilon_{n'} + \frac{q_\parallel^2}{2m^*} \right)^2 \right] - F_{-1/2}\left[\frac{\varepsilon_f - \varepsilon_n}{T_e} - \frac{m^*}{2q_\parallel^2 T_e}\left(\omega + \varepsilon_{n'} - \varepsilon_n + \frac{q_\parallel^2}{2m^*} \right)^2 \right] \right\} \tag{13}$$

$$\Pi_2^{1D} = -\frac{m^*}{|q_z|} \left[f\left(\frac{q_z^2}{8m^*} + \tfrac{1}{2}(\varepsilon_{m,l} + \varepsilon_{m',l'} - \omega) + \frac{m^*}{2q_z^2}(\omega + \varepsilon_{m,l} - \varepsilon_{m',l'})^2 \right) - f\left(\frac{q_z^2}{8m^*} + \tfrac{1}{2}(\varepsilon_{m,l} + \varepsilon_{m',l'} + \omega) + \frac{m^*}{2q_z^2}(\omega + \varepsilon_{m,l} - \varepsilon_{m',l'})^2 \right) \right] \tag{14}$$

where

$$F_{-1/2}(x) = \frac{1}{\sqrt{\pi}} \int_0^\infty dy \, y^{-1/2} [1 + \exp(y - x)]^{-1}$$

is the Fermi–Dirac integral of order $-1/2$ and

$$f(x) = [1 + \exp(x)]^{-1}$$

is the Fermi–Dirac function.

We assume that electrons are coupled with GaAs bulk phonons since the bulk phonons are a good approximation for transport studies in quantum wells and quantum wires [29, 30]. The sum over λ includes longitudinal acoustic modes (deformation potential and piezoelectric interaction), transverse acoustic modes (piezoelectric interaction) and longitudinal optic modes (deformation potential and polar interaction).

The electron inverse mobility, $1/\mu = E/v_d = -f(v_d)/N_e e v_d$, comprises contributions from electron impurity scatterings, $1/\mu_i$, and electron–phonon couplings, $1/\mu_p$, i.e. $1/\mu = 1/\mu_i + 1/\mu_p$.

3. Transport results and discussions

In the numerical calculation, we consider 21 subbands for quantum wires and seven subbands for quantum slabs, together with all the intrasubband and intersubband scatterings. The material parameters of GaAs used in the calculation are the same as those used in [9]. For the purposes of comparisons between results in systems of different lateral confinement, we let $d_1 = d_2 = d$ and the electron bulk density n_3 is the same for all systems in the calculation. Furthermore, we assume that all systems have the same density of background impurities, which is determined so that the resulting linear low-temperature ($T = 2$ K) mobility due to background impurities in bulk GaAs material with electron density $n_3 = 3.18 \times 10^{23}$ m^{-3} have the value μ_i^0. Two cases for impurities, $\mu_i^0 = \infty$ and $\mu_i^0 = 10$ m^2 V^{-1} s^{-1}, are considered in this paper.

3.1. The dependence on electron density

As is well known, when electrons are highly degenerate at low temperature, transitions can happen only between states near the Fermi level in the range of $k_B T_e$. The properties of electrons are mainly determined by the position of the Fermi energy in the energy band and the density of states therein. In low-dimensional electron systems (quantum wells or quantum wires), the energy band splits into subbands because of lateral confinement. As the Fermi energy increases from the bottom of the ground subband, it is expected that the mobility of electrons will change periodically with a period of the energy interval between two adjacent subbands. At low temperatures, the piezoelectric and deformation potential interactions between acoustic phonons and electrons are the prominent scattering mechanisms in GaAs in the limit $\mu_i^0 = \infty$. Since the frequencies of acoustic phonons are limited by the Debye frequency, and the square matrix element of the piezoelectric interaction $|M(q)|^2_{\text{piezo}}$ has a q^{-2} dependence, the mobility is strongly limited when the Fermi energy locates at each subband bottom, especially in a quantum wire where the density of states diverges at the subband bottom. This is the reason why linear mobilities of low-dimensional electrons (curve 2 for wells and curve 3 for wires) are lower than that of bulk electrons (curve 1) at low electron density, as shown in figure 1(*a*), where we plot the electron bulk density (n_3) dependence of linear and high-field mobility in dimensionally different systems with $\mu_i^0 = \infty$ at a lattice temperature $T = 10$ K. With increasing electron density, the linear mobilities of low-dimensional electrons gases fluctuate around the value of bulk material. Once the Fermi energy reaches a new subband the mobilities begin to decrease abruptly. The oscillation of phonon-limited mobility is similar to the impurity-limited mobility found by Hu and O'Connell [24] and to the recent experimental results of Ismail and co-workers [3].

With increasing temperature, electron transitions can happen in a larger range of energy, and the marked subband effect is smoothed, as illustrated in figure 1(*b*), where the lattice temperature $T = 77$ K and only linear mobility is shown (full curve for the wire, broken curve for the well and dotted curve for the bulk material). Another feature in figure 1(*b*), different from figure 1(*a*), is that the electron mobility in quantum wires is on average lower than that in quantum wells, and they are both lower than that in bulk material at low electron density ($n_3 < 2.5 \times 10^{24}$ m^{-3} in figure 1(*b*)). This result, different from early expectations [14, 22], comes from the optic phonon contribution and can be interpreted as follows. Considering only the remote ionic impurity scattering mechanism in EQL, and neglecting form factor effects, Sakaki estimated the electron mobility at low temperature in quantum wire structures, and predicted that a much higher mobility may be obtained in one-dimensional systems than those in two- or three-dimensional systems at low

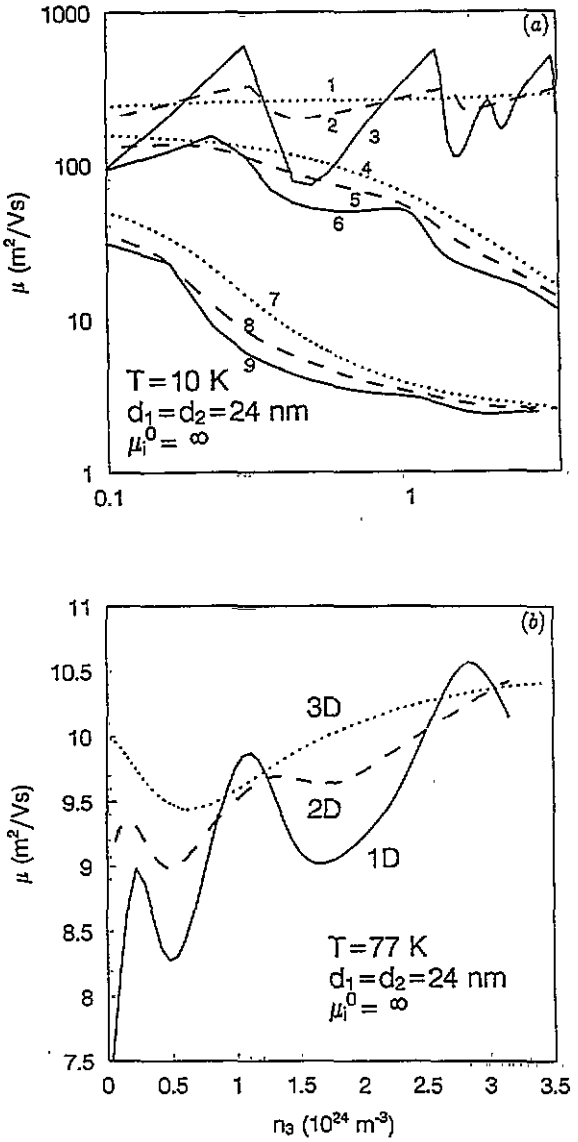

Figure 1. Phonon-limited electron mobilities ($\mu_i^0 = \infty$) against carrier density at different lattice temperatures. Dotted curves: mobility of bulk material; broken curves: mobility of quantum wells; full curves: mobility of quantum wires. (*a*) $T = 10$ K. Results at electron drift velocities $v_d = 0$ (1, 2, 3); $v_d = 7.94 \times 10^4$ m s^{-1} (4, 5, 6) and $v_d = 1.59 \times 10^5$ m s^{-1} (7, 8, 9). (*b*) Linear mobilities at $T = 77$ K.

temperature, because of the reduction of phase space and the number of available final states during the scattering processes. However, the case is different for electron–optic-phonon scattering mechanisms. First, the limitation of final states is not the most important for scattering since the electrons are not strongly degenerate at higher temperatures. Second, in a three-dimensional scattering process, the three-dimensional momentum must be conserved ($q_i = q_f + q_p$) as well as the energy, but in quantum wires, for example, only in-line momentum need be conserved ($q_{iz} = q_{fz} + q_{pz}$). Thus for definite in-line momentum

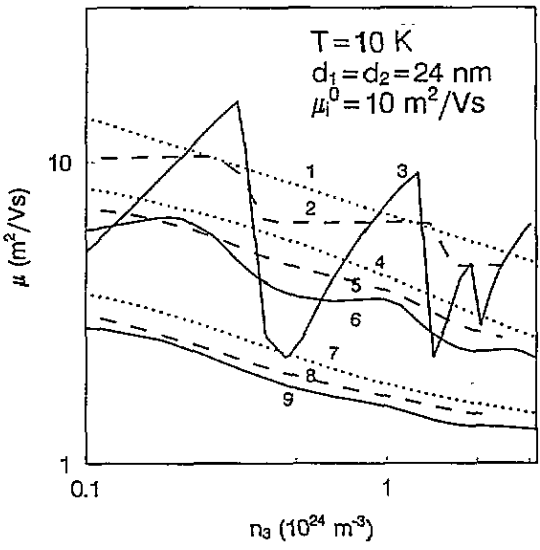

Figure 2. Electron mobilities ($\mu_i^0 = 10$ m^2 V^{-1} s^{-1}) against carrier density at a lattice temperature $T = 10$ K. Dotted curves represent results of bulk material; broken curves represent results of quantum wells; full curves represent results of quantum wires. The electron drift velocities: curves (1, 2, 3) for $v_d = 0$; (4, 5, 6) for $v_d = 7.94 \times 10^4$ m s^{-1} and (7, 8, 9) for $v_d = 1.59 \times 10^5$ m s^{-1}.

transfer $q_{iz} - q_{fz}$, there are more phonons that can be devoted in quantum wires.

It is worth noting that the mobility minimum in a three-dimensional electron system at electron density $n_3 = 5.5 \times 10^{23}$ m^{-3} (figure 1(*b*)) comes from the onset of the polar optic phonon scattering where the Fermi energy equals the optic phonon energy ($E_F = \Omega_{LO}$).

In figure 1(*a*) we have also calculated the non-linear mobility against carrier density at drift velocity $v_d = 7.94 \times 10^4$ m s^{-1} (curves 4, 5 and 6) and $v_d = 1.59 \times 10^5$ m s^{-1} (curves 7, 8 and 9). At high electric field, both increased electron temperature and increased drift velocity suppress the mobility oscillation because of the extension of the electron energy spectrum, the crossover from a low-dimensional system to a three-dimensional system can be observed as the electron density increases.

Figure 2 shows the same relationship as figure 1(*a*), but with $\mu_i^0 = 10$ m^2 V^{-1} s^{-1}. Under the influence of background impurities, the subband effect on linear mobility of low-dimensional systems is obvious, and the linear mobility decreases on average with the increase of carrier density, which is different from the behaviour of the phonon-limited mobility in figure 1(*a*).

3.2. The dependence on electric field

Phonon-limited mobility against electric field curves in systems of various dimensionality and confinement are plotted in figure 3. In figure 3(*a*), where the width of the quantum well and the diameter of the quantum wire are both $d = 24$ nm, and the electron bulk density $n_3 = 3.18 \times 10^{23}$ m^{-3}, we find that the dimensionality and the subband effect on electron mobility tend to vanish at very high electric field. But under low or intermediate electric field, the mobility of different systems can show distinct features. At a low lattice temperature ($T = 2$ K), the electron mobility of the quantum wire, which can be one order of magnitude greater than that of the bulk material under low fields, is smaller than that

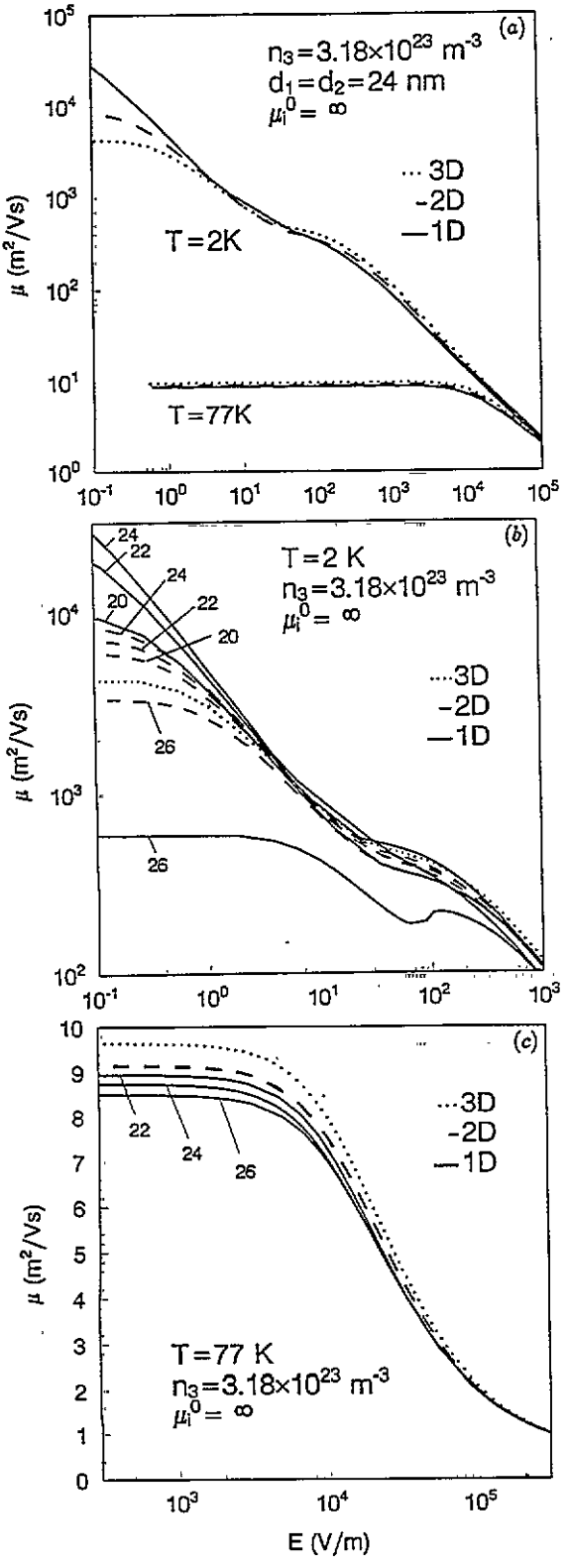

Figure 3. Electric field dependence of phonon-limited mobilities ($\mu_i^0 = \infty$) in one-, two- and three-dimensional systems at lattice temperatures $T = 2$ K and $T = 77$ K. (*b*) and (*c*) show the results of various lateral confinement in detail where the numbers beside curves denote the diameter (in nm) of the quantum wire or the width of quantum well.

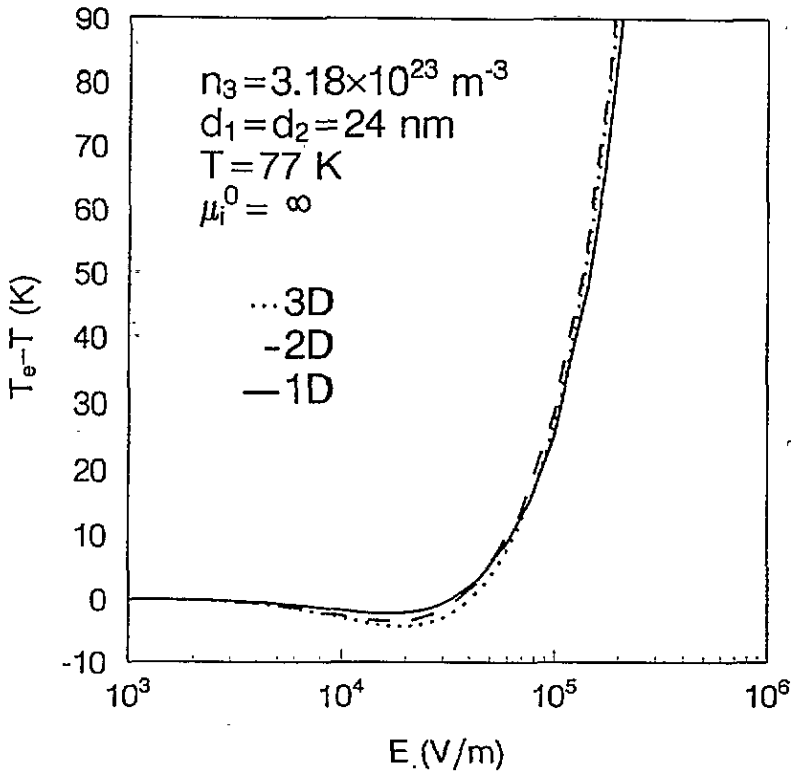

Figure 4. The difference between electron and lattice temperature as a function of electric field at lattice temperature $T = 77$ K when $\mu_i^0 = \infty$.

of the bulk material or quantum well under intermediate fields when optic phonons begin to contribute to the mobility. At a high lattice temperature $T = 77$ K, low-dimensional mobility is nearly the same as the bulk mobility. This is in conflict with the previous expectation that low-dimensional electron gases can greatly increase the mobility [16, 22]. In fact, the obvious increase of mobility in one-dimensional systems can only happen in some optimum conditions at low temperature, as shown in figures 1 and 2.

In figure 3(b) we plot in detail low lattice temperature ($T = 2$ K) phonon-limited mobility against electric field in systems with a variety of confinement and dimensionality. The outstanding thing here is that the curve of the quantum wire of diameter $d_1 = 26$ nm is significantly lower than other curves over a large range of the electric field, which gives rise to the fact that the Fermi level here just locates above the bottom of the second subband. In quantum wells the electron mobility is also strongly limited when the well width $d_2 = 26$ nm, but its behaviour is not so marked because of the difference in the state density spectrum. The other curves of low-dimensional systems arrange according to the strength of confinement at low electric field, but are rearranged at high field, which reflects the hot electron and drift electron effect on mobility. Figure 3(c) shows in detail the electric field dependence of phonon-limited electron mobility in systems of various dimensionality and lateral confinement at lattice temperature $T = 77$ K.

The increment of electron temperature $T_e - T$ against electric field E in one-, two- and three-dimensional systems with $\mu_i^0 = \infty$ at a lattice temperature $T = 77$ K is plotted in

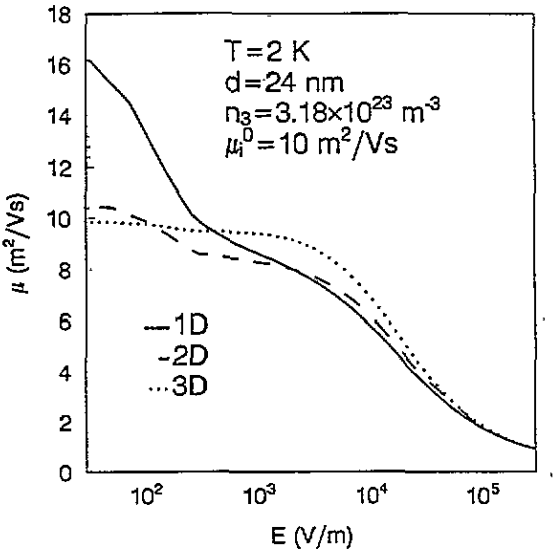

Figure 5. Electron mobilities of one-, two- and three-dimensional systems against electric field plotted when $\mu_i^0 = 10$ m^2 V^{-1} s^{-1} at lattice temperature $T = 2$ K.

figure 4. A cooling effect is obvious in all systems when the electron field is lower than $E = 4 \times 10^4$ V m^{-1} and has the same electric field dependence.

Figure 5 shows the electric field dependence of electron mobility at a lattice temperature $T = 2$ K and lateral extension $d = 24$ nm when $\mu_i^0 = 10$ m^2 V^{-1} s^{-1}. Linear mobilities in low-dimensional systems are higher than those in the bulk material. While in intermediate electric fields ($E \sim 10^3 - 10^5$ V m^{-1}), the electron mobility in one- or two-dimensional systems becomes lower than that in three-dimensional systems due to the influence of higher subbands. When the electric field is higher than 10^5 V m^{-1}, subband and dimensionality effects disappear.

Electron and lattice temperature difference against electron drift velocity is illustrated in figure 6 under the same conditions as figure 5. At low electric fields, electrons in the quantum wire only occupy the ground subband with a Fermi energy under the second subband, and have a much higher electron temperature. But under intermediate electric fields, the electron temperature of the 1D system is lower than other systems when more subbands are occupied by electrons.

3.3. The dependence on temperature

In figure 7(a), we investigate the lattice temperature dependence of phonon-limited mobility ($\mu_i^0 = \infty$) for electrons of different drift velocity and dimensionality. For linear electron mobilities (curves 1, 2 and 3 in figure 7(a)), the lower the dimensionality of the system, the higher the mobility when $d_1 = d_2 = 24$ nm and $n_3 = 3.18 \times 10^{23}$ m^{-3}, but for non-linear mobilities (curves 4, 5 and 6 for $v_d = 7.94 \times 10^4$ m s^{-1} and curves 7, 8 and 9 for $v_d = 1.59 \times 10^5$ m s^{-1}) the situation turns out to the contrary. Because of subband effects [26], high-field mobility in a quantum wire becomes the lowest among these systems. Figure 7(b) compares the electron temperature dependence of mobility at lattice temperatures $T = 2$ K and $T = 77$ K with that of linear mobility ($T = T_e$). Here we show that the electron drift velocity can strongly influence the electron mobility, and the experimental

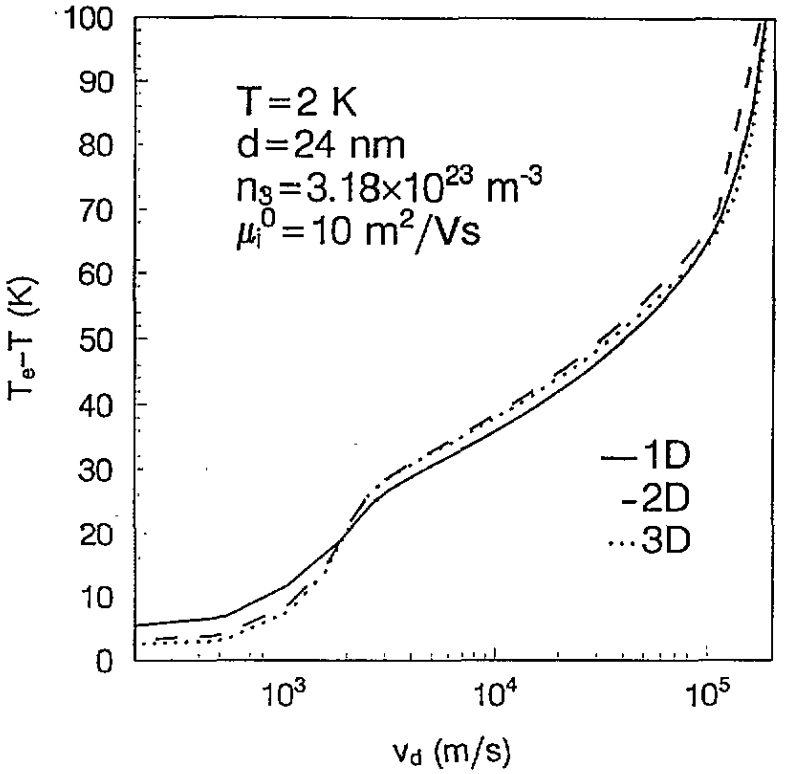

Figure 6. The difference between electron and lattice temperature in various systems shown as a function of drift velocity when $\mu_i^0 = 10$ m^2 V^{-1} s^{-1} at lattice temperature $T = 2$ K.

method of determining the electron temperature T_e in high electric fields by measuring electron high-field mobility and using the relation between linear mobility and temperature (when $T = T_e$) may lead to large deviations. The inset denotes the corresponding drift velocity (v_d) against electron temperature (T_e).

3.4. The effects of lateral confinement

Linear electron mobilities as a function of lateral dimension $d = d_1 = d_2$ are illustrated in figure 8(a) for a lattice temperature $T = 77$ K and in figure 8(b) for a lattice temperature $T = 300$ K where the chain curve is the result of EQL in quantum wires. Electron mobilities in quantum wires and quantum wells do not exceed the value in the bulk material, but approach it as the lateral confinement becomes weak, and crossover from low-dimensional systems to a three-dimensional system can be observed. The result of EQL overestimated the electron mobility even in quantum wires of diameter as small as 12 nm. Because 21 subbands in quantum wires are not enough to calculate the electron transport when the diameter is large, the calculated mobility of 1D systems increases abnormally in figure 8(b) when $d_1 > 30$ nm and we conclude that, to estimate correctly the electron mobility at high temperature in low-dimensional systems, it is important to take enough subbands into account.

Although so far there have not been enough available experimental data on electron mobility in long quantum wires for a direct quantitative comparison between theoretical

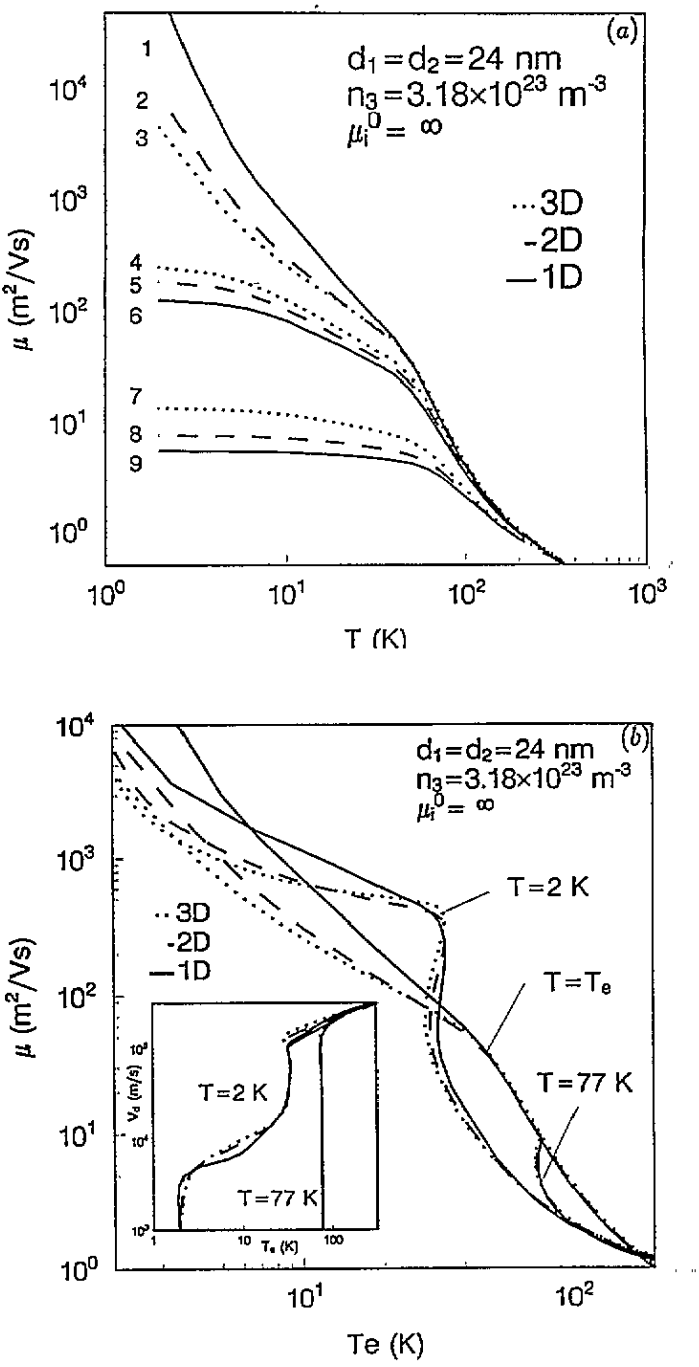

Figure 7. Electric mobilities plotted as a function of lattice temperature (*a*) and electron temperature (*b*). Electron drift velocities in (*a*) are $v_d = 0$ for curves 1, 2, 3; $v_d = 7.94 \times 10^4$ m s^{-1} for curves 4, 5, 6 and $v_d = 1.59 \times 10^5$ m s^{-1} for curves 7, 8, 9. The inset in (*b*) shows the electron drift velocity against electron temperature at lattice temperature $T = 2$ K and $T = 77$ K.

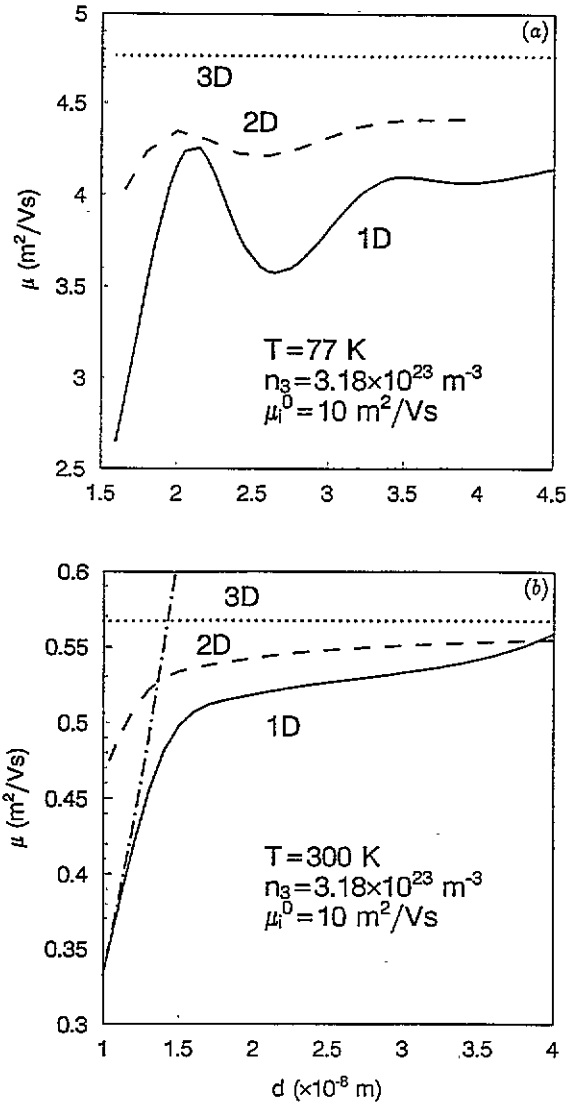

Figure 8. Linear electron mobilities as a function of lateral confinement (d) at temperature (a) $T = 77$ K and (b) $T = 300$ K when $\mu_i^0 = 10$ m^{2}V^{-1} s^{-1}. The chained curve in (b) is the result of EQL in quantum wires.

and experimental results, some features discussed in this paper have been shown by recent measurements [3–5]. The theoretical prediction of mobility modulation by electron lateral confinement has been observed by Ismail and co-workers [3]. In addition, Sawaki and co-workers [4] showed that, in the case of the same linear mobility for both Q1DEG and Q2DEG, the non-linear mobility of Q1DEG becomes lower than that of Q2DEG when the electric field increases. At low temperature ($T = 1.8$ K), Hauser and co-workers [5] found that Q1DEG and Q2DEG with identical low-field mobility have different intermediate-field mobility but the same high-field mobility, and the mobility increases with weakening lateral confinement.

4. Conclusion

In summary, we have estimated electron mobilities in quantum wires and quantum wells using the Lei–Ting balance equation transport theory. The results were compared with that in bulk materials. At low lattice temperature, a significant increase of linear mobility in quantum wires may obtain in some optimum conditions. Unlike the conclusion given by Leburton and co-workers [16, 22] we did not find a much higher electron mobility in quantum wires than in quantum wells and bulk materials at high temperature. Our results are consistent with those given by Mickevicius and co-workers [27]. At high electric field, non-linear mobility in low-dimensional systems shows very different behaviour from linear mobility.

References

[1] Stormer H L, Pfeiffer L N, Baldin K W and West K W 1990 *Phys. Rev.* B **41** 1278
[2] Hasko D G, Potts A, Cleaver J R A, Smith C G and Ahmed H 1988 *J. Vac. Sci. Technol.* B **6** 1849
[3] Ismail K, Antoniadis D A and Smith H I 1989 *Appl. Phys. Lett.* **54** 1130
[4] Sawaki N, Sugimoto R and Hori T 1993 *Proc. 8th Conf. on Hot Electron Systems* to be published
[5] Hauser M, Gornik E, Wirner C, Baur M, Böhm G and Weimann G 1993 *Proc. 8th Conf. on Hot Electron Systems* to be published
[6] Watt M, Sotomayor Torres C M, Arnot H E G and Beaumout S P 1990 *Semicond. Sci. Technol.* **5** 285
[7] Ridley B K 1991 *Rep. Prog. Phys.* **54** 169
[8] Ando T, Fowler A B and Stern F 1982 *Rev. Mod. Phys.* **54** 437
[9] Lei X L, Birman J L and Ting C S 1985 *J. Appl. Phys.* **58** 2270
Lei X L, Zhang J Q, Birman J L and Ting C S 1986 *Phys. Rev.* B **33** 4382
[10] Hirakawa K and Sakaki H 1986 *Appl. Phys. Lett.* **49** 889; 1986 *Phys. Rev.* B **33** 8291
[11] Yokoyama K and Hess K 1986 *Phys. Rev.* B **33** 5595; 1986 *J. Appl. Phys.* **59** 3798
[12] Kawamura T and Das Sarma S 1992 *Phys. Rev.* B **45** 3612
[13] Ghosal A, Chattopadhyay D and Bhattacharyga A 1986 *J. Appl. Phys.* **59** 2511
[14] Sakaki H 1980 *Japan J. Appl. Phys.* **19** L735
[15] Leburton J P 1984 *J. Appl. Phys.* **56** 2850
[16] Leburton J P 1992 *Phys. Rev.* B **45** 11 022 -
[17] Fasol G and Sakaki H 1993 *Phys. Rev. Lett.* **70** 3643
Fasol G 1991 *Appl. Phys. Lett.* **59** 2430; 1992 *Appl. Phys. Lett.* **61** 831
[18] Campos V B and Das Sarma S 1992 *Phys. Rev.* B **45** 3898
Das Sarma S, Campos V B, Stroscio M A and Kim K W 1992 *Semicond. Sci. Technol.* **7** B60
[19] Vickers A J 1992 *Phys. Rev.* B **46** 13 313
[20] Guillemot C, Clérot F and Regreny A 1992 *Phys. Rev.* B **46** 10 152
[21] Yamada T and Sone J 1989 *Phys. Rev.* B **40** 6265
[22] Briggs S and Leburton J P 1988 *Phys. Rev.* B **38** 8163; 1989 *Phys. Rev.* B **39** 8025
[23] Semelius B E, Berggren K F, Tomak M and McFadden C 1985 *J. Phys. C; Solid State Phys.* **18** 225
[24] Hu G Y and O'Connell R F 1991 *Phys. Rev.* B **43** 12 341
[25] Bockelmann U and Bastard G 1990 *Phys. Rev.* B **42** 8947
[26] Wang X F and Lei X L 1993 *Phys. Status Solidi* **175** 433; 1993 *Phys. Rev.* B **47** 16 612
[27] Mickevicius R, Mitin V V, Kim K W and Stroscio M A 1992 *Semicond. Sci. Technol.* **7** B299
[28] Lei X L and Ting C S 1984 *Phys. Rev.* B **30** 4809; 1985 *Phys. Rev.* B **32** 1112
Lei X L and Horing N J M 1992 *Int. J. Mod. Phys.* B **6** 805
[29] Tsuchiya T and Ando T 1992 *Semicond. Sci. Technol.* **7** B73
[30] Wang X F and Lei X L 1994 *Phys. Rev.* B **49** 4780